https://doi.org/10.5194/gmd-2022-222
Preprint. Discussion started: 16 December 2022

Geoscientific Model Development Discussions
Open Access

DynQual v1.0: A high-resolution global surface water quality model

Edward R. Jones[1,*], Marc F.P Bierkens[1,2], Niko Wanders[1], Edwin H. Sutanudjaja[1], Ludovicus P.H van Beek[1], Michelle T.H. van Vliet[1]

[1]Department of Physical Geography, Faculty of Geosciences, Utrecht University, Utrecht, The Netherlands.

[2]Deltares, Unit Soil and Groundwater Systems, Utrecht, The Netherlands

* Correspondence to: e.r.jones@uu.nl

Abstract

Maintaining good surface water quality is crucial to protect ecosystem health and for safeguarding human water use activities. Yet, our quantitative understanding of surface water quality is mostly predicated upon observations at monitoring stations that are highly limited in space and fragmented across time. Physically-based models, based upon pollutant emissions and subsequent routing through the hydrological network, provide opportunities to overcome these shortcomings. To this end, we have developed the dynamical surface water quality model (DynQual) for simulating water temperature (Tw) and concentrations of total dissolved solids (TDS), biological oxygen demand (BOD) and fecal coliform (FC) with a daily timestep and at 5 arc-minute (~10km) spatial resolution. Here, we describe the main components of this new global surface water quality model and evaluate model performance against in-situ water quality observations. Furthermore, we describe both the spatial patterns and temporal trends in TDS, BOD and FC concentrations for the period 1980–2019, also attributing the dominant contributing sectors. The model code is available open-source (https://github.com/UU-Hydro/DYNQUAL) and we provide global datasets of simulated hydrology, Tw, TDS, BOD and FC at 5 arc-minute resolution with a monthly timestep (https://doi.org/10.5281/zenodo.7139222). This data has potential to inform assessments in a broad range of fields, including ecological, human health and water scarcity studies.

https://doi.org/10.5194/gmd-2022-222
Preprint. Discussion started: 16 December 2022

1. Introduction

Maintaining good surface water quality is important for protecting ecosystem health and ensuring human access to safe water resources for a diverse range of sectoral needs (Van Vliet et al., 2021; Jones et al., 2022). For example, high organic pollution can reduce oxygen availability and can lead to the suffocation of aquatic organisms (Sirota et al., 2013), while pathogen pollution represents a potential health risk for people exposed to this water. The consumption of contaminated drinking water can lead to the transmission of diseases such as cholera, dysentery and polio leads, which cause an estimated 485,000 deaths annually (Prüss-Ustün et al., 2019). Another example is salinisation of water resources, which can both limit irrigation water use (Thorslund et al., 2022) and threaten freshwater biodiversity (Velasco et al., 2019) where species cannot tolerate elevated salinity concentrations. Similarly, increased water temperatures can disrupt energy production (Van Vliet et al., 2016), while also providing more favourable conditions for cyanobacterial blooms that can lead to hypoxia that disrupt freshwater habitats (Smucker et al., 2021).

Human activities, both directly and indirectly, cause changes in surface water quality relative to ambient ('pristine') conditions. Indirectly, altered precipitation patterns and the increased frequency of hydro-meteorological extremes that result from human-induced climate change can lead to fundamental changes in the hydrological regime (Wanders and Wada, 2015; Gudmundsson et al., 2021). Lower water levels due to altered seasonality patterns or droughts reduce the stream dilution capacity, which increases the proportion of streamflow originating from (polluted) point sources (Wright et al., 2014; Luthy et al., 2015; Ehalt Macedo et al., 2022). Both of these factors increase river water contamination, threatening both the safe usability of water and environmental health. Climate change is also altering the thermal regime of rivers (Van Vliet et al., 2013), with higher temperatures also causing dissolved oxygen depletion (Ozaki et al., 2003).

More directly, sectoral activities generate return flows - water that is extracted for a specific purpose but is not consumed (evaporated) in the process – but which has changed in composition as a result of the water use activity (Sutanudjaja et al., 2018; Jones et al., 2021). For example, the composition of domestic wastewaters will reflect the various household water uses, including organic and fecal contamination from human waste (Wwap, 2017) and elevated nutrient concentrations from household chemicals and laundry detergents (Van Puijenbroek et al., 2019). The re-introduction of these flows back to the environment represent a significant source of pollutant loadings that degrade river water quality (Jones et al., 2022). Collection and treatment of these flows, before their re-introduction to the environment, can help to minimise the impact on surface water quality (Jones et al., 2022). Yet, these processes can be economically expensive to establish and operate, and hence collection and treatment infrastructure not ubiquitous worldwide (Jones et al., 2021; Jones et al., 2022).

Water quality is an integral part of the Sustainable Development Agenda, cross-cutting almost all Sustainable Development Goals (SDGs). Despite widespread recognition of its importance, water quality monitoring data is still severely lacking in several world regions – particularly Africa and Central Asia (Damania et al., 2019). Furthermore, in regions where observation data is available, data is often sparse in both space and time. Water quality models offer opportunities to overcome these limitations (Hofstra et al., 2013; Beusen et al., 2015; UNEP, 2016; Van Vliet et al., 2021). As opposed to statistical models which heavily rely on observed water quality data, physical models simulate the emission and transport of pollutant loadings along the river network directly based on climatic, hydrological and socio-economic input data. This makes physically-based model approaches especially advantageous when predicting water quality in ungauged catchments and for projecting water quality under future (uncertain) climatic and socio-economic developments (Wanders et al., 2019).

A spatially and temporally detailed assessment of multiple water quality constituents at the global scale is lacking. Furthermore, only a few studies have quantitatively evaluated temporal dynamics and

https://doi.org/10.5194/gmd-2022-222
Preprint. Discussion started: 16 December 2022

Geoscientific Model Development
Discussions

trends in water quality over extended time periods, particularly considering changes in factors that drive higher pollutant emissions (e.g. population growth, industrialisation) relative to factors that abate pollutant emissions (e.g. wastewater treatment). Lastly, no studies have assessed the spatio-temporal patterns in the specific sectoral activities that are driving patterns in surface water quality worldwide.

Here, we present a high-spatiotemporal resolution surface water quality model (henceforth *DynQual*), which can currently be used to simulate water temperature (Tw), and concentrations of total dissolved solids (TDS) to represent salinity, biological oxygen demand (BOD) to represent organic pollution and fecal coliform (FC) as a coarse indicator for pathogen pollution. All simulations are provided at a daily timestep with a spatial resolution of 5x5 arc-minutes (approx. 10km at the equator). DynQual considers a wide range of hydro-climatic and socio-economic drivers, spanning across the major contributing pollutant sources. The high spatio-temporal resolution of DynQual (i.e. 5 arc-min and daily timestep), combined with these features, allows the model to address scientific questions that are not currently possible using existing surface water quality models. For example, while previous work has compared pollutant loads (masses) originating from different sources at aggregated spatial scales (i.e. basin or subbasin level), the impact on in-stream concentrations - which is also dependent upon spatio-temporal variability in dilution capacity and in-stream decay processes – has not been assessed.

The objectives of this study are to: 1) introduce a new open-source global surface water quality model and evaluate model performance; 2) assess spatial patterns and trends in surface water quality, focussing on total dissolved solids (TDS), biological oxygen demand (BOD) and fecal coliform (FC) concentrations for the period 1980 – 2019; and 3) demonstrate additional model capabilities by assessing the sector-specific contributions towards surface water pollution across both space and time.

https://doi.org/10.5194/gmd-2022-222
Preprint. Discussion started: 16 December 2022

2. DynQual – model description

2.1 General overview

The newly developed DynQual model builds on the modelling framework of DynWat, a global water temperature model that solves the energy-water balance to simulate daily water temperature (Tw) and ice thickness (Van Beek et al., 2012; Wanders et al., 2019). A full model description including the energy balance equations and the representation of ice cover, floodplains, channel roughness and lakes and reservoirs within DynWat is available in published literature (Wanders et al., 2019). DynQual further includes the impact of heat dumps produced in thermoelectric powerplants (Van Vliet et al., 2012a; Van Vliet et al., 2021) on water temperature. In addition to water temperature, DynQual simulates daily in-stream concentrations of three water quality constituents, namely, total dissolved solids (TDS), biological organic matter (BOD) and fecal coliform (FC), which are of key social and environmental relevance (Van Vliet et al., 2021) (Figure 1).

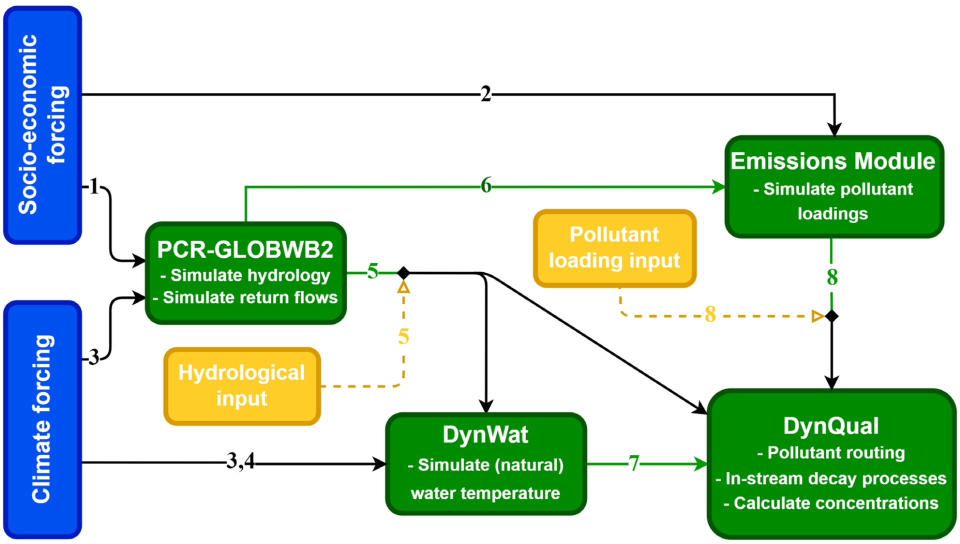

Socio-economic forcing
1. *Domestic gross and net water demand (m day^{-1}); industry gross and net water demand (m day^{-1}); livestock gross and net water demand (m day^{-1})*
2. *Population numbers; livestock numbers; urban fraction; thermo-electric power return flows (m^3 s^{-1}); excretion rates (g or cfu day^{-1}); mean effluent concentrations (mg l^{-1} or cfu 100ml^{-1})*

Climate forcing
3. *Air temperature (°C); precipitation (m day^{-1}); potential evapotranspiration (m day^{-1})*
4. *Solar radiation (W m^{-2}); annual average air temperature (°C); vapour pressure (kPa); cloud cover (%); sunlight hours (hours day^{-1})*

Hydrological data
5. *Baseflow or groundwater discharge (m day^{-1}); interflow (m day^{-1}); direct or surface runoff (m day^{-1})*
6. *Manufacturing return flows (m^3 day^{-1}); irrigation return flows (m^3 day^{-1}); urban surface runoff (m^3 day^{-1})*
7. *Water temperature (°C)*

Pollutant loading data
8. *Anthropogenic temperature loading (MW); TDS loading (g day^{-1}); BOD loading (g day $^{-1}$); FC loading (10^6 cfu day^{-1})*

Figure 1. Overview of the required input data for running DynQual in different model configurations. Runs coupled with PCR-GLOBWB2 require socio-economic[1] and climatic[3,4] forcing data as standard, with options to either 1) calculate loads based on additional socio-economic[2] and simulated hydrological[6] data ; or 2) provide pollutant loadings directly as input data[7]. Offline runs require both hydrological[5] and pollutant loadings[7] input data to be provided directly.

We also offer two options for running DynQual, either: 1) in a stand-alone configuration with user-defined hydrological input from any land surface or hydrological model, or 2) one-way coupled with the global hydrological and water resources model PCR-GLOBWB2 (Sutanudjaja et al., 2018). A full model description of PCR-GLOBWB2 including detailed information on the model structure, individual modules (meteorology, land surface, groundwater, surface water routing and water use) and validation of hydrological output is available in published literature (Sutanudjaja et al., 2018).

In both configurations of DynQual, pollutant loadings can be prescribed directly (akin to a forcing). Alternatively, when running DynQual coupled with PCR-GLOBWB2 (or another hydrological model that includes water withdrawals and return flows), pollutant loadings can be simulated within the model runs by providing only simple input data (SI Section 1). A schematic for DynQual, also specifying the required input data associated with different model configurations, is displayed (Figure 1). By providing these options, we allow for flexibility – allowing pollutant loadings to be directly imposed on the model facilitates users to calculate loadings using their preferred methodology and assumptions; whereas the option to calculate pollutant loadings within the model run enables users to simulate water quality without any pre-processing requirements but with their preferred input datasets. When simulating pollutant loadings within model runs, it is also possible to quantify the contribution and relative importance of different water use sectors to the spatial patterns and temporal trends in surface water quality.

2.2 Water quality equations

2.2.1 Water temperature (Tw)

Water temperature (Tw) is simulated by solving the surface water energy balance using the DynWat model as basis (Van Beek et al., 2012; Wanders et al., 2019). In addition to solving the surface water energy balance, DynWat also accounts for surface water abstraction, reservoirs, riverine flooding and the formation of ice (Wanders et al., 2019). Here, we further develop DynWat to include advected heat flows from thermoelectric powerplants, as per the method described in van Vliet et al., (2012; 2016). The modelling equations for Tw incorporated into DynQual are shown in Eq. [1] and are fully elaborated on in previous work (Van Beek et al., 2012; Van Vliet et al., 2012a; Van Vliet et al., 2016; Wanders et al., 2019).

$$\rho_w C_p \frac{\partial (hT_w)}{\partial t} = \rho_w C_p \frac{\partial (vT_w)}{\partial x} + H_{tot} + \rho_w C_p \int_{x=0}^{dx} q_s T_s + \frac{Tw_{pow_n}}{h * w * dx}$$

$$H_{tot} = S_{in}(1 - a_w) + L_{in} - L_{out} - H - LE$$

$$Tw_{pow_n} = \rho_w * C_p * RF_{pow,n} * \Delta T_{pow\_rf}$$

[1]

Where t is time , x is location along the drainage network, T_w is water temperature (K), C_p is the specific heat capacity of water (4,190 J kg^{-1} K^{-1}), ρ_w is the density of fresh water (1000 kg m^{-3}), h is the stream water depth (m), v is the velocity of water (m s^{-1}), H_{tot} is the heat flux at the air-water interface, S_{in} is the incoming shortwave radiation (J m^{-2} s^{-1}), $1 - a_w$ is the reflected shortwave radiation (J m^{-2} s^{-1}), L_{in} is the incoming longwave radiation (J m^{-2} s^{-1}), L_{out} is the outgoing longwave radiation (J m^{-2} s^{-1}), H is the sensible heat flux (J m^{-2} s^{-1}), LE is the latent heat flux (J m^{-2} s^{-1}), q_s are the lateral water fluxes from land to stream (m s^{-1}), T_s is the temperature of lateral water fluxes (K), Tw_{pow_n} is the heat dump from thermo-electric powerplants (J s^{-1}), C_p is the specific heat capacity of water (4,190 J kg^{-1} K^{-1}), ρ_w is the density of fresh water (1000 kg m^{-3}), RF_{pow} is the return flows of cooling water (m^3 s^{-1}), ΔT_{pow_rf}

https://doi.org/10.5194/gmd-2022-222
Preprint. Discussion started: 16 December 2022

Geoscientific Model Development Discussions

is the difference in water temperature between the return flows and ambient river water (K), w is the stream width (m) and dx is the distance between gridcell n and the upstream gridcell $n-1$ (m).

2.2.2 Conservative (TDS) and non-conservative (BOD, FC) substances

Our modelling strategy for total dissolved solids (TDS), biological oxygen demand (BOD) and fecal coliform (FC) is a mass balance approach assuming transport by advection only, whereby sector-specific loadings – masses of pollutants generated from a particular human activity in a given time period – are accumulated from all contributing sectors and routed through the global stream network until outflow to the ocean (Thomann and Mueller, 1987; Chapra and Pelletier, 2004; Voß et al., 2012; UNEP, 2016; Van Vliet et al., 2021).

TDS is modelled as a conservative substance, while BOD and FC are modelled as non-conservative substances that include first-order decay processes (Voß et al., 2012; Reder et al., 2015; UNEP, 2016; Van Vliet et al., 2021). Our approach for both the conservative and non-conservative substances assumes instantaneous and full mixing of all streamflow and return flows in each grid cell. As per most water quality models, DynQual simulates water quality per individual gridcell over a consecutive series of discrete time periods (Loucks and Beek, 2017). Each gridcell represents a volume element, which is in steady-state conditions within each time period, which also contains a (fully-mixed) pollutant mass (Figure 2). In each consecutive timestep, there is an associated volume of water and mass of pollutant that flows into the gridcell from upstream and that flows out of the gridcell to the downstream gridcell. For non-conservative substances, there are also gridcell-specific in-stream decay processes that influence the total mass of pollutant in each sub-time interval. DynQual simulates these transport and decay processes with a sub-daily interval (Δt in seconds), the length of which is determined with respect to channel characteristics and discharge (SI Section 2 & SI Eq. [8]).

https://doi.org/10.5194/gmd-2022-222
Preprint. Discussion started: 16 December 2022

Geoscientific Model Development Discussions

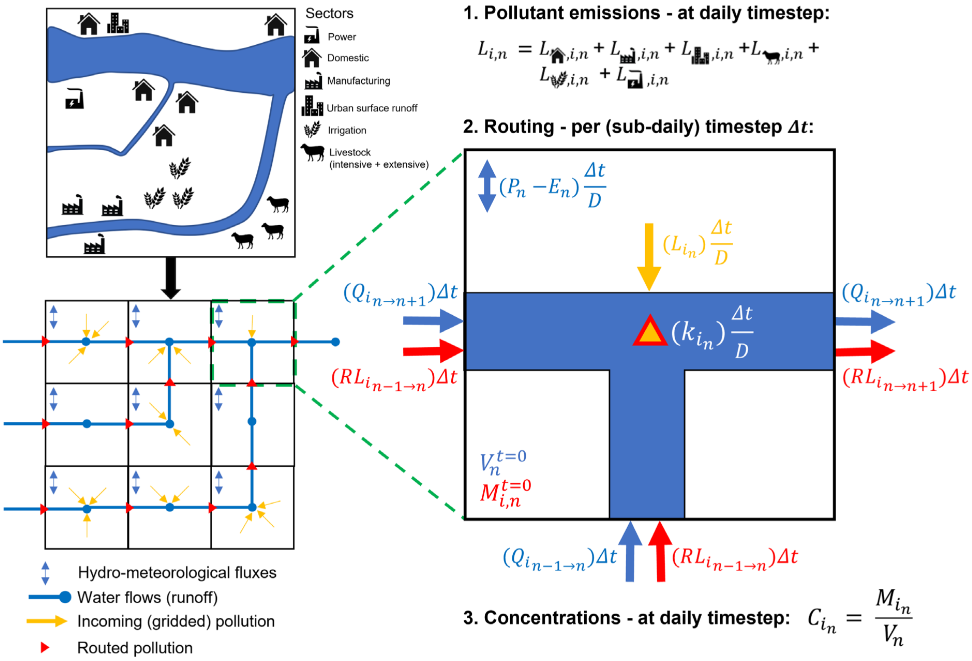

Figure 2. Schematic overview of DynQual, including a translation of local hydrological and socio-economic situation (a) into a local drain direction (LDD) map that includes hydrological and pollutant fluxes (b) and a representation of the gridcell based processes (pollutant emission calculation, routing procedure and computation of pollutant concentrations) in an individual DynQual gridcell (c). $C_{i,n}$ is the concentration of pollutant i (e.g. mg l^{-1}), while $M_{i,n}$ is the total mass pollutant i (e.g. g) and V_n is the channel storage (m^3), all in gridcell n. $V_n^{t=0}$ is the volume of channel storage from the previous timestep (m^3), while $Q_{i_{n-1\rightarrow n}}$ and $Q_{i_{n\rightarrow n+1}}$ is the discharge (m^3 s^{-1}) into and out of gridcell n, respectively, per timestep Δt. $M_{i,n}^{t=0}$ is the mass of pollutant i from the previous timestep, while $RL_{i_{n-1\rightarrow n}}$ and $RL_{i_{n\rightarrow n+1}}$ are the loadings of pollutant i (e.g. g s^{-1}) that are routed into and out of gridcell n, respectively, per timestep Δt. $L_{i,n}$ are the combined local loadings of pollutant i (e.g. g day^{-1}) in gridcell n, which is the sum of loadings from all contributing sectors and urban surface runoff. $k_{i,n}$ is decay coefficient that depends upon pollutant i (-). D is the length of a day in seconds (i.e. 86 400 s day^{-1}), while Δt is the length of sub-timestep (s) which is linked to the internal routing regime within DynQual & PCR-GLOBWB2. P_n is precipitation (m^3 day^{-1}) and E_n is evapotranspiration (m^3 day^{-1}), with these terms included as an example of gridcell-specific hydrological fluxes. For a more detailed overview of the hydrological fluxes within a gridcell we refer to the PCR-GLOBWB 2 documentation (Sutanudjaja et al., 2018).

The pollutant concentration at each subsequent time interval ($t + \Delta t$) is calculated following Eq. [2]. It should be noted that, while we simulate the terms of this equation with a sub-daily timestep interval, DynQual only reports concentrations in the final sub-daily interval of each day. This is due to the lack of sub-diurnal input data, for efficient data storage and the lack of relevance of such high-resolution simulations with respect to our large-scale modelling approach.

$$C_{i.n}^{t+\Delta t} = \frac{M_{i,n}^{t+\Delta t}}{V_n^{t+\Delta t}} + BG_{i,n} \qquad [2]$$

https://doi.org/10.5194/gmd-2022-222
Preprint. Discussion started: 16 December 2022

Geoscientific Model Development
Discussions

Where $\mathrm{C}_{\mathrm{i.n}}^{\mathrm{t}+\Delta t}$ and $\mathrm{M}_{\mathrm{i,n}}^{\mathrm{t}+\Delta t}$ is the concentration and mass, respectively, of pollutant *i* in gridcell *n* at the consecutive time interval ($t+\Delta t$), whereas $\mathrm{V}_{\mathrm{n}}^{\mathrm{t}+\Delta t}$ is the volumetric channel storage (m^3) in this gridcell in the same interval. $\mathrm{V}_{\mathrm{n}}^{\mathrm{t}+\Delta t}$ is simulated directly within PCR-GLOBWB2, accounting for the initial storage, discharge into and out of gridcell *n* over the time interval Δt and gridcell specific hydrological fluxes including precipitation and evapotranspiration (Sutanudjaja et al., 2018). $\mathrm{M}_{\mathrm{i,n}}^{\mathrm{t}+\Delta t}$ is simulated by solving the mass balance equation for pollutant *i* and accounting for in-stream decay processes following Eq. [3]. $BG_{i,n}$ represents the background concentration of pollutant *i* in gridcell *n*. For TDS, these are calculated based on minimum observed EC-converted to TDS observations (Walton, 1989) contained in a new global salinity dataset (Thorslund and Van Vliet, 2020). Conversely, $BG_{BOD,n}$ and $BG_{FC,n}$ are assumed to be negligible, relative to the mass of pollution produced by anthropogenic activities.

$$M_{i,n}^{t+\Delta t} = \left(M_{i,n}^{t=0} + \left(\Sigma(RL_{i_{n-1\to n}}) - RL_{i_{n\to n+1}} + \frac{L_{i_n}}{D}\right)\Delta t\right) * e^{-k_{i,n}(\frac{\Delta t}{D})} \qquad [3]$$

Where, at the subsequent timestep interval ($t+\Delta t$), each gridcell *n* contains the mass of pollutant *i* from the previous timestep ($M_{i.n}^{t=0}$) plus the pollutant load (mass second^{-1}) that has been transported from the immediately (adjacent) upstream gridcell(s) ($RL_{i_{n-1\to n}}$) and minus the pollutant load (mass s^{-1}) that has been transported downstream ($RL_{i_{n\to n+1}}$) in the time interval Δt (s). $L_{i,n}$ represents the daily influx of pollutant loadings produced into gridcell *n* (mass day^{-1}), which are added to the stream in equal increments per sub-daily timestep Δt (s) relative to the total length of a day D in seconds (i.e. 86,400 s day^{-1}). Our approach for adding local pollutant loadings in equal increments per sub-daily timestep is necessary as we lack information regarding the (sub-diurnal) timing at which pollution enters the stream network.

$k_{i,n}$ represents a pollutant *i* and gridcell *n* specific decay rate (day^{-1}). While we model TDS as a conservative substance (i.e. $k_{TDS,n} = 0$), we determine the first-order degradation rate of BOD (k_{BOD_n}) as a function of water temperature (Eq. [4]) and of FC (k_{FC_n}) as function of water temperature, solar radiation and sedimentation (Eq. [5]). Decay is implemented directly into DynQual by assuming decay to occur at an equal rate over the course of a day ($\frac{\Delta t}{D}$). This assumption is necessary because we do not have sub-daily input data for some terms of the decay equations, such as water temperature (Tw) and incoming solar radiation (I_o).

$$k_{BOD,n} = k(20) * \Theta^{(Tw_n - 20)} \qquad [4]$$

Where $k(20)$ is a first-order degradation rate coefficient at 20°C (day^{-1}) assumed at 0.35 (Van Vliet et al., 2021); Tw_n is the water temperature (^{O}C) in gridcell n and Θ is a temperature correction assumed to be 1.047 as per previous assessments (Wen et al., 2017; Van Vliet et al., 2021).

$$k_{FC_n} = k_d \Theta^{(Tw_n - 20)} + k_s \frac{I_o}{k_e H}\left(1 - e^{-k_e H}\right) + \frac{v}{H} \qquad [5]$$

Where k_d is dark inactivation (day^{-1}); Θ is a temperature correction; Tw_n is the water temperature (^{O}C) in gridcell *n*; k_s is sunlight inactivation (m^2 W^{-1}); I_o is the surface solar radiation (W m^{-2}); k_e is an attenuation coefficient (m^{-1}); H is stream depth (m) and v is the settling velocity (m day^{-1}). Parameter values (

Table *1*) and mean basin average total suspended solids (Beusen et al., 2005) are based off previous fecal coliform modelling studies (Reder et al., 2015).

Table 1. Assumed parameter values for fecal coliform modelling

Variable	Unit	Value
k_d	day^{-1}	0.82
Θ	-	1.07
k_s	m^2 W^{-1}	0.0068
k_e	m^{-1}	0.0931TSS + 0.881
v	m day^{-1}	1.656

2.3 Pollutant loadings

In both model configurations (stand-alone and one-way coupled to PCR-GLOBWB2), user-calculated pollutant loadings can be directly imposed on the model (akin to a forcing). Users can pre-calculate pollutant loadings using their preferred methodology, and subsequently route these through the global stream network and account for in-stream decay processes using the DynQual model framework in order to calculate in-stream pollutant concentrations. Pollutant loadings that are prescribed to DynQual directly should have a daily temporal resolution (e.g. g day^{-1} or cfu day^{-1}).

Alternatively, when running DynQual coupled with PCR-GLOBWB2, pollutant loadings with a daily temporal resolution can be simulated within the model runs, requiring only simple input data (see Figure 1 and SI Section 1). This option is beneficial for users who do not have pre-calculated pollutant loadings. Furthermore, this option may be useful for those interested in scenario modelling, as input files related to different scenarios can be altered to reflect alternative climate and socioeconomic conditions. In this set-up, DynQual calculates and routes pollutant loadings individually and combined for the main water use sectors (domestic, manufacturing, livestock and irrigation) and from urban surface runoff at 5 arc-minute spatial resolution. For this, gridded datasets on human population numbers, livestock population numbers and urban fractions are required. Additionally, estimates of per capita excretion rates of pollutants (humans, livestock) and mean effluent pollutant concentrations (manufacturing, urban surface runoff and irrigation) are required. A detailed explanation of how pollutant loadings are calculated within DynQual is provided in SI Section 1, including the equations (SI Eqs. [1-7]) and all parameter estimates (SI Table S1-S7) .

3. Model demonstration

3.1 Model run setup and validation

DynQual is run for the time period 1980 – 2019 using W5E5 forcing data (Cucchi et al., 2020; Stefan et al., 2021) in the online configuration with PCR-GLOBWB2, using the simplified kinematic wave routing option (Sutanudjaja et al., 2018). We focus our analysis on TDS, BOD and FC, as results for Tw have been displayed extensively in previous work (Wanders et al., 2019). Pollutant loadings of TDS, BOD and FC are calculated within the model run at the daily timestep. Both the meteorological forcing data and input data used for simulating pollutant loadings used in this study are accessible through links provided in the code and data availability statement. Furthermore, we also provide the model code and full input data required for running an example catchment (Rhine basin) in the code and data availability statement.

https://doi.org/10.5194/gmd-2022-222
Preprint. Discussion started: 16 December 2022

Geoscientific Model Development
Open Access
Discussions

Model simulations were compared to observations from surface water quality monitoring stations worldwide at daily temporal resolution. Observed data was obtained from a variety of state-of-the-art databases. Tw and BOD data was downloaded from the GRQA (Global River Water Quality Archive) (Virro et al., 2021), which combines data from various sources including GEMStat (Global Freshwater Quality Database) (UNEP, 2020), GLORICH (GLObal River CHemistry) (Hartmann et al., 2014) and WQP (Water Quality Portal) (Read et al., 2017). Electrical conductivity (EC) data was obtained from a global salinity database (Thorslund and Van Vliet, 2020), additionally supplemented with GEMStat data (UNEP, 2020), and converted to TDS (see SI Section 3). FC data was obtained from GEMStat (UNEP, 2020), additionally supplemented with data from the National Water Information System (NWIS) from the United States Geological Survey (USGS) (U.S. Geological Survey, 2016).

Water quality monitoring data covers the entire modelled time period (1980 – 2019) and includes a far greater number of observations than in previous surface water quality modelling validation procedures (SI Section 3; Table S8). It should be noted that there is an uneven distribution in data availability, with more observations in Europe and the United States for all water quality constituents. We evaluate model performance statistically based on the root-mean-square-error normalised with the mean (nRMSE), providing a comparable indication of prediction errors across the different water quality constituents. The distribution of nRMSE values (SI Eq. [9]), sub-divided by annual average river discharge, is displayed in Figure 3. Overall, the strongest validation performance is found for Tw, followed by TDS, BOD and then FC. Across all water quality constituents, model simulations tend to represent the observed data best in larger streams (>100 m^3 s^{-1}), particularly for BOD and FC. The influence of spatial mismatches between monitoring station locations and model simulations is especially important in smaller streams, where concentrations are more sensitive to natural dilution capacity (i.e. water availability) and variabilities in pollutant source contributions. More detailed information regarding the validation process and results, including spatial patterns and time-series (Figure S2 – S6), is presented in the SI (Section 3) and previous work (Jones et al., 2022).

https://doi.org/10.5194/gmd-2022-222
Preprint. Discussion started: 16 December 2022

Geoscientific Model Development
Discussions

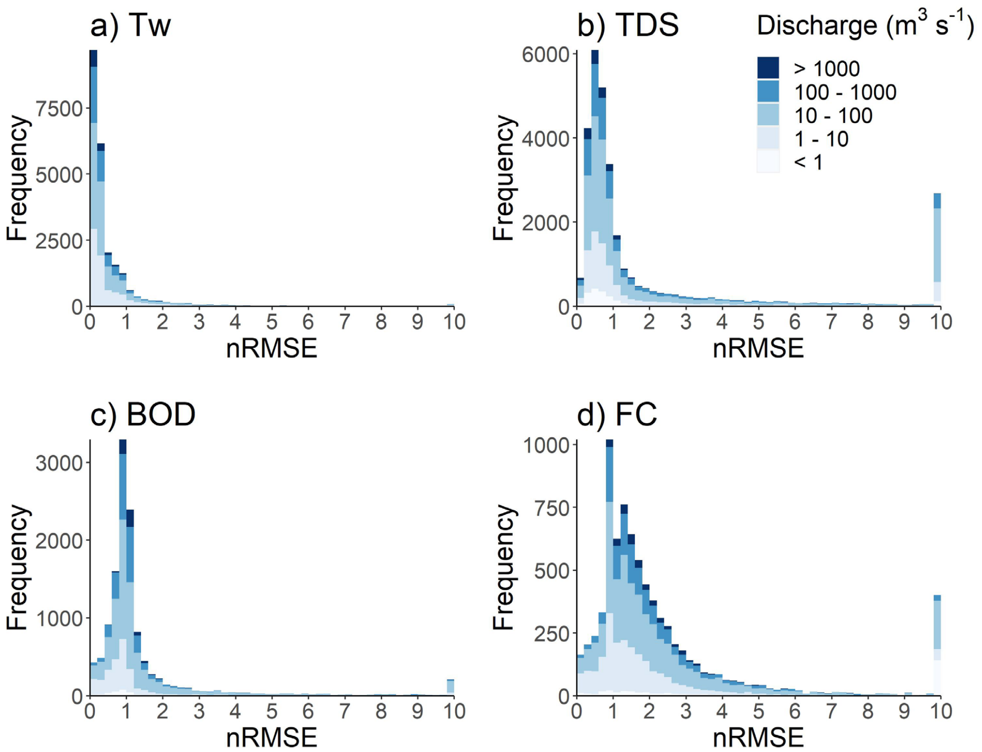

Figure 3. Normalised root mean square error (nRMSE) for a) water temperature (Tw), b) total dissolved solids (TDS), c) biological oxygen demand (BOD) and d) fecal coliform (FC) simulations.

3.2 Spatial patterns

The spatial patterns in TDS (Figure 4), BOD (Figure 5) and FC (Figure 6) concentrations show substantial variations both within and across world regions, driven by different sectoral activities (Figure 7). The dilution capacity of rivers is also a major determinant of in-stream concentrations. Averaged at the annual time-scale this is particularly evident for BOD and FC where the large dilution capacity of some major rivers is sufficient to dilute concentrations to relatively low levels, despite often being fed by more polluted tributaries. However, it should also be noted that both river discharges and in-stream concentrations can exhibit substantial intra-annual variability (Figure 8), thus pollutant hotspots and the magnitude of pollutant levels must also be considered at finer temporal scales than presented here.

https://doi.org/10.5194/gmd-2022-222
Preprint. Discussion started: 16 December 2022

Geoscientific Model Development
Discussions

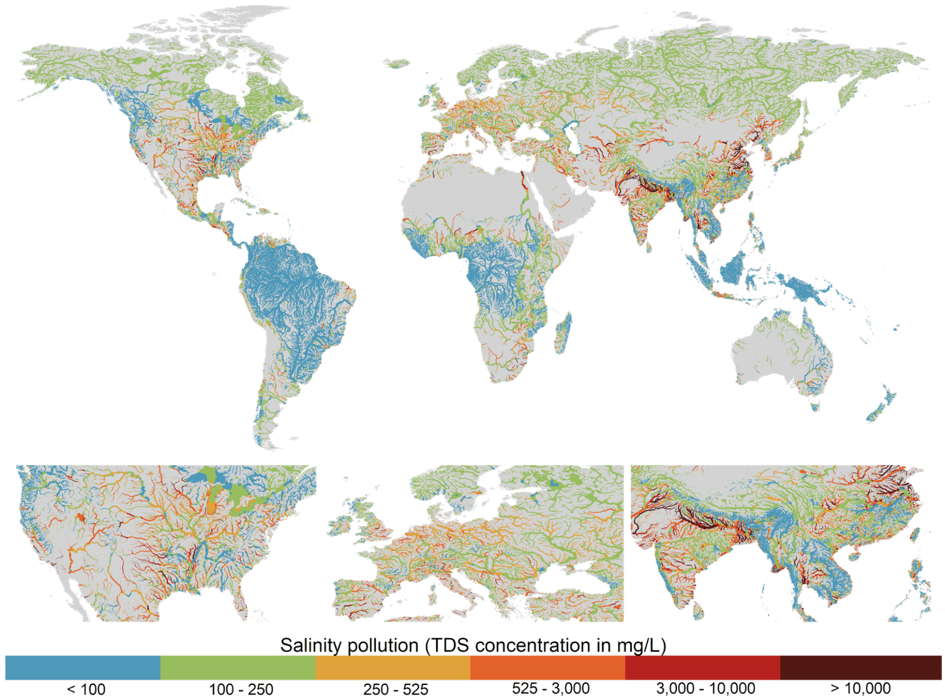

Figure 4. Annual average total dissolved solids (TDS) concentrations for the period 2010 – 2019. Plotted for rivers with > 10 $m^3 s^{-1}$ annual average discharge.

TDS concentrations show strongly regional patterns, with key hotspots of salinity pollution located in south-east Asia (Pakistan and northern India) and eastern China, and to a lesser degree across the United States and Europe (Figure 4). High TDS concentrations in south-east Asia are predominantly driven by the irrigation sector and the presence of saline soils (Figure 7a). The irrigation sector is also an important driver of TDS pollution in eastern China, where the contribution from manufacturing activities are also significant (Figure 7a). The manufacturing sector is the dominant contributor of TDS pollution across most of North America and Western Europe, accounting for >75% of in-stream pollutant loadings in almost all major river segments (Figure 7a). Aside from the lower Nile, where salinity pollution is predominantly from the manufacturing sector, the domestic sector is the key source of (non-natural) TDS loadings in Africa. However it should be noted that, aside from in the lower Nile, TDS concentrations are generally quite low across most of Africa (Figure 4; Figure 7a).

https://doi.org/10.5194/gmd-2022-222
Preprint. Discussion started: 16 December 2022

Geoscientific Model Development Discussions

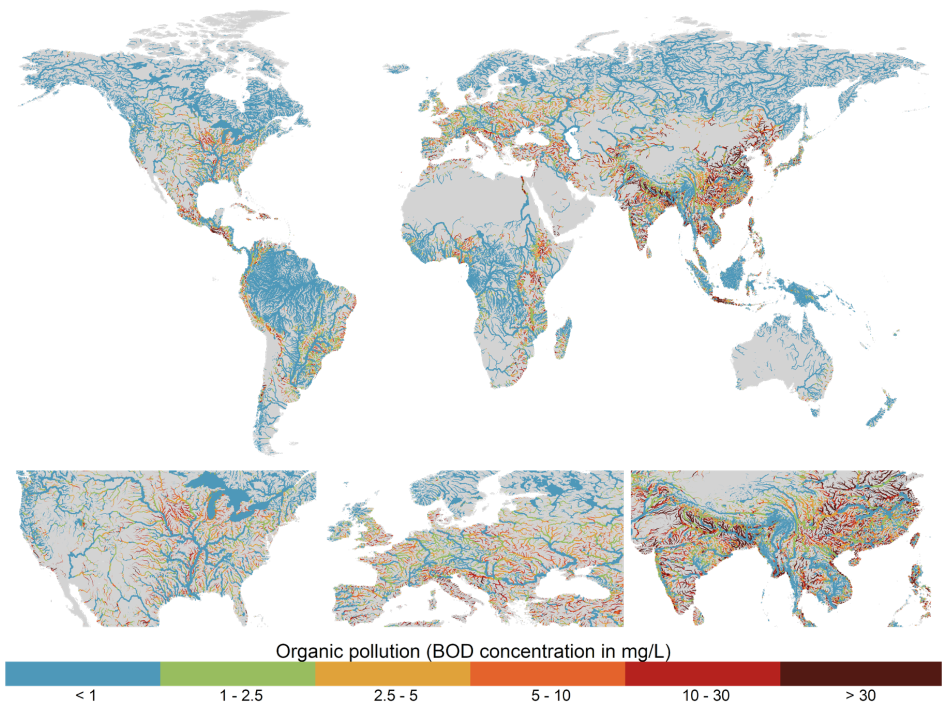

Figure 5. Annual average biological oxygen demand (BOD) concentrations for the period 2010 – 2019. Plotted for rivers with > 10 m^3 s^{-1} annual average discharge.

While BOD concentrations show considerable diversity across the major world regions, a substantial proportion of river segments across populated areas of all continents experience moderate-to-high organic pollution (Figure 5). There are clear spatial patterns in the dominant sectoral activities contributing BOD loadings worldwide, and it also evident that BOD pollution in most world regions is driven by a combination of multiple sectors opposed to from an individual dominant activity (Figure 7b). Across Europe in particular, which sector is dominant varies both spatially and temporally and the contribution from the dominant sector is typically <50% (Figure 7b). The manufacturing sector is the most significant source of BOD pollution across rivers in the United States, however the relative contribution commonly falls in the 20 – 50% or 50 – 75% categories (Figure 7b). In the most polluted world regions, south and south-east Asia, typically the domestic sector is dominant. However, there are also significant contributions from manufacturing and extensive livestock activities (Figure 5; Figure 7b). Lastly, while its influence is highly localized, urban surface runoff can also represent an important source of BOD pollution in heavily urbanised gridcells across all world regions.

https://doi.org/10.5194/gmd-2022-222
Preprint. Discussion started: 16 December 2022

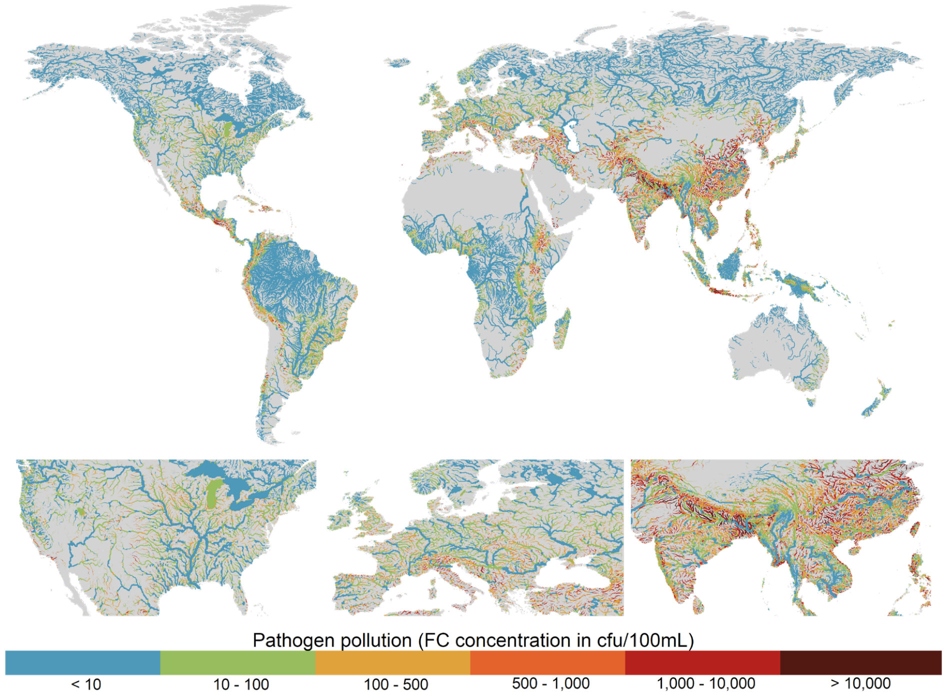

Figure 6. Annual average fecal coliform (FC) concentrations for the period 2010 – 2019. Plotted for rivers with > 10 m^3 s^{-1} annual average discharge.

FC pollution is particularly high across south and south-east Asia, with more localised hotspots found in parts of western Latin America, southern Europe, Middle East and eastern Africa (Figure 6). Similar to BOD pollution, a large proportion of stream segments in south and south-east Asia are heavily polluted, with typically only rivers with extremely high dilution capacities appearing in the lower concentration classes. In this region, the domestic sector is predominantly responsible for FC pollution (commonly > 75%), attributed to large urban populations coupled with a large proportion of domestic wastewater being inadequately treated (Figure 7c). In countries with high municipal wastewater collection and treatment rates, such as in Europe, the relative influence of livestock activities tends to be larger. While manufacturing activities remain the dominant source of FC pollution in North America, despite relatively high wastewater treatment rates, the percentage contribution is typically <50% and livestock activities also represent an important source of FC loadings (Figure 7c). Despite variable municipal wastewater collection and treatment rates across Latin America, livestock activities appear to dominate FC loadings outside of the Amazon basin (Figure 7c). This can be attributed to very high livestock numbers (particularly cattle), combined with the fact that the most of the large urban settlements (and thus domestic FC pollutant loadings) in South America are located in the coastal zone. As such, pollution from the domestic and manufacturing sectors typically enter the river network at downstream locations causing localised pollution before outflow to the ocean.

https://doi.org/10.5194/gmd-2022-222
Preprint. Discussion started: 16 December 2022

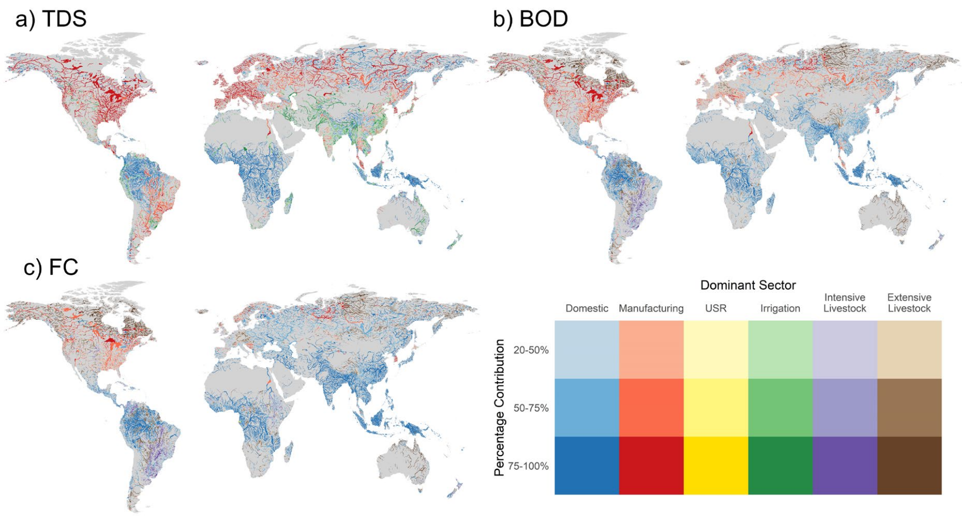

Figure 7. Dominant sectoral activity contributing towards a) total dissolved solids (TDS), b) biological oxygen demand (BOD) and c) fecal coliform (FC) pollution averaged over 2010 – 2019. Plotted for rivers with > 10 $m^3 s^{-1}$ annual average discharge.

In addition to the significant spatial variability in surface water concentrations of TDS, BOD and FC, there is also substantial intra-annual variability (Figure 8). In the model, intra-annual variability can occur due temporal variations in: 1) pollutant loadings; 2) water availability (i.e. dilution capacity) and 3) in-stream decay processes. As TDS concentrations are modelled using a conservative approach, fluctuations in concentrations throughout the year occur due to variability in pollutant loadings and water availability only. In regions where sectoral emissions of TDS are very low, such as in the high-latitudes and Amazon basin, intra-annual fluctuations in TDS concentrations are very low as well, reflecting background concentration levels (Figure 8a). Conversely, the largest fluctuations occur in regions with large variations in streamflow (i.e. dilution capacity) and/or where sectoral water use and hence TDS emissions are strongly seasonal. This is particularly evident in the Indian subcontinent (India, Pakistan, Bangladesh) where there is both large fluctuations in streamflow coupled with highly seasonal irrigation water demands. In regions where TDS loadings are dominated by sectors that contribute more constant pollutant loadings throughout the year, most notably the domestic (Africa) and manufacturing (North America, Western Europe) sectors, intra-annual variations in TDS concentrations are more reflective of hydrological variability.

For non-conservative constituents (BOD and FC), additional variation in intra-annual concentrations also occurs as a result of decay rates, which are a function of water temperature (BOD and FC), sedimentation (FC only) and solar radiation (FC only). As the dominant sectors generating BOD (domestic and manufacturing) and FC loadings (domestic) in most world regions show relatively stable emissions to the stream network throughout the year, intra-annual variability in concentrations are mostly resulting from variations in streamflow and/or decay rates. Compared to TDS (Figure 8a), average annual fluctuations in BOD (Figure 8b) and FC (Figure 8c) tend to occur to a greater extent and are more widespread in space. Regions that display the largest intra-annual variations in water temperature coincide with those areas where fluctuations in both BOD and FC are much greater than for TDS, most notably in the United States and Eastern China.

https://doi.org/10.5194/gmd-2022-222
Preprint. Discussion started: 16 December 2022

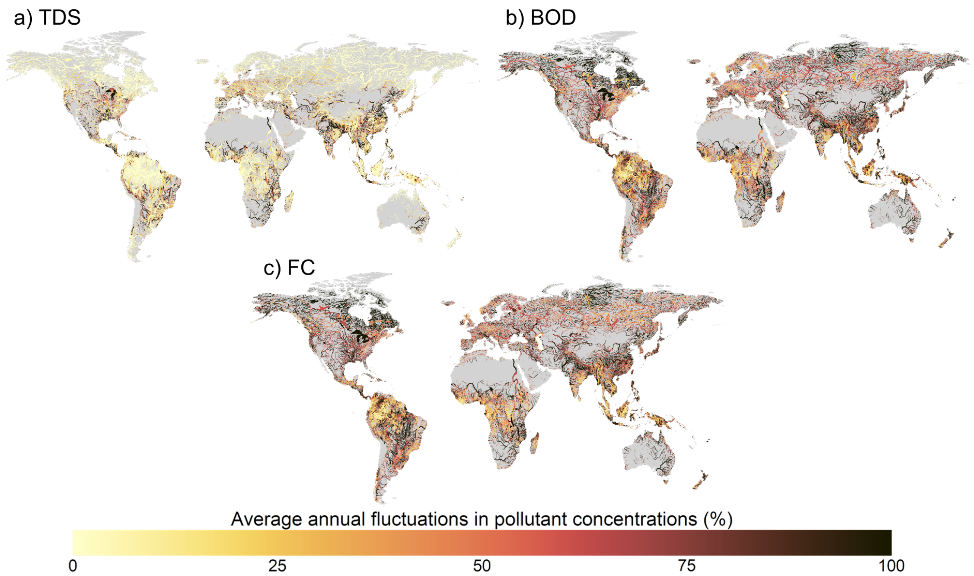

Figure 8. Average annual fluctuations in a) total dissolved solids (TDS), b) biological oxygen demand (BOD) and c) fecal coliform (FC) concentrations for the period 2010 – 2019. Fluctuations are computed as the coefficient of variation, and are expressed as an average percentage per year. Plotted for rivers with > 10 m^3 s^{-1} annual average discharge.

3.3 Trends

We also considered long-term trends in TDS, BOD and FC concentrations over the simulated period (1980 - 2019) (Figure 9). TDS concentrations in most world regions are either relatively constant or show relatively upwards gradual trends. Only small areas show decreasing TDS trends (Figure 9a). Typically, where TDS concentrations are increasing, the trend has been driven mainly by expansions in manufacturing or irrigation activities. Comparatively, trends in BOD (Figure 9b) and FC (Figure 9c) concentrations are larger in magnitude and exhibit substantially more spatial variation across the major world regions. Regionally, the strongest increases in BOD and FC are found in sub-Saharan Africa, where wastewater treatment rates are low, and south Asia, where the rate of population growth and economic development has significantly outstripped expansions in wastewater treatment infrastructure. Strong increasing trends are also found across most of Latin America, where a significant proportion of collected wastewater does not undergo wastewater treatment (UNEP, 2016; Jones et al., 2021). BOD and FC concentrations across North American rivers have typically remained relatively constant, or exhibit small decreasing trends. Strong decreasing trends are found across Europe, including the Danube and Rhine basins. In all world regions, the influence of reservoirs on BOD and FC concentrations is also evident, with increased water volumes (i.e. dilution) coupled with longer residence times (i.e. greater decay) reducing BOD and FC concentrations at these specific locations.

https://doi.org/10.5194/gmd-2022-222
Preprint. Discussion started: 16 December 2022

Geoscientific Model Development
Discussions
Open Access
EGU

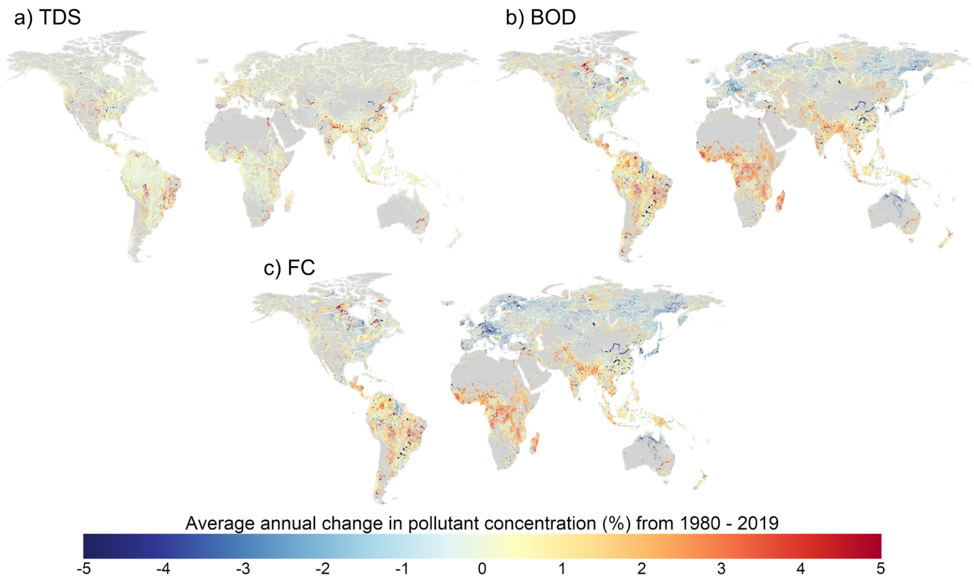

Figure 9. Average annual percentage changes in a) total dissolved solids (TDS), b) biological oxygen demand (BOD) and c) fecal coliform (FC) concentrations for the period 1980 – 2019. Plotted only for rivers with > 10 m^3 s^{-1} annual average discharge.

Complementary to the spatial analysis, we considered the proportion of population inhabiting gridcells exhibiting different trends in pollutant concentrations, aggregated by geographical region and economic classification (Figure 10). It should be noted that trends (Figures 8 and 9) are not indicative of the degree of pollution directly, and thus should also be considered with respect to in-stream concentrations (Figures 3-6). Changes in TDS concentrations in the most populated areas worldwide are typically low, with increases of 0 – 1% most common across all geographical regions (Figure 10a). Conversely, strong regional patterns are evident for BOD (Figure 10b) and FC (Figure 10c) concentrations. Particularly in Sub-Saharan Africa and Southern Asia, BOD and FC concentrations in populated locations have been almost exclusively increasing. Over half of the population of Sub-Saharan Africa live in areas where BOD and FC concentrations have increased (on average) by >2% per year from 1980 – 2019. Conversely, in Western Europe, trends in BOD and FC have been negative for areas where 60% of the population lives.

When aggregating trends by country-specific economic classifications, trends in TDS, BOD and FC pollutant concentrations all display a clear correlation with level of economic development (Figure 10). For the water quality constituents considered, the strongest and most widespread decreases in pollutant concentrations have been experienced by 'high-income' countries, while 'low-income' countries have experienced the greatest and most widespread degree of water quality degradation. These patterns are particularly clear for FC, where approximately 60% of the population in 'high-income' countries live in gridcells displaying negative trends in FC concentrations, compared to 50%, 25%, and 10% in 'upper-middle', 'lower-middle' and 'low-income' countries, respectively. Furthermore, in the 'low-income' countries, 50% of the population live in areas where FC concentrations have increased (on average) by 2% each year from 1980 to 2019.

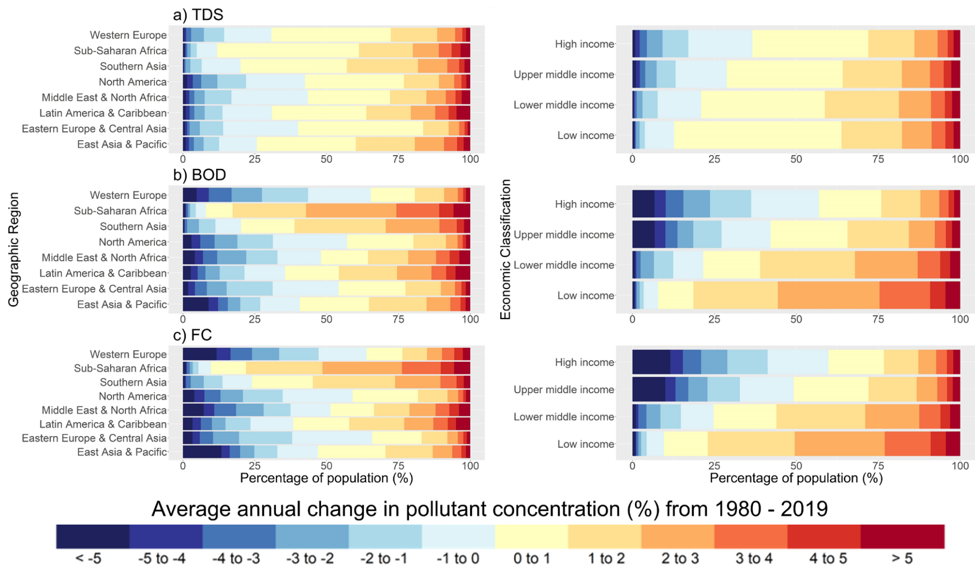

Figure 10. Average annual percentage changes in a) total dissolved solids (TDS), b) biological oxygen demand (BOD) and c) fecal coliform (FC) concentrations for the period 1980 – 2019. Results are displayed for the proportion of population (%) inhabiting gridcells exhibiting different trends in pollutant concentrations, aggregated by geographical region (left) and economic classification (right).

To further illustrate both trends and temporal variations in TDS, BOD and FC, we present time-series of in-stream concentrations delineated by sector-specific contributions for three selected locations (Figure 11). TDS concentrations in all three locations display an increasing trend since 1980, with the manufacturing sector being the dominant source of loadings in the Danube and Hudson. Conversely, TDS loadings from the irrigation sector is the main determinant of salinity concentrations in the Karnaphuli, which also exhibits substantial intra-annual variations attributed to high seasonality. Average BOD and FC concentrations in the Karnaphuli river approximately doubled from 1980 to 2019, predominantly due to increasing loadings from the domestic sector, while also exhibiting high seasonal variability. Relatively small trends in BOD and FC concentrations are simulated in the Hudson, mostly driven by the domestic sector but also with contributions from manufacturing activities and urban surface runoff. Conversely, strong reductions in BOD and FC concentrations are found for the Danube (Figure 11). These trends are predominantly driven by decreasing pollutant loadings from the domestic and manufacturing sectors, as expansions in wastewater treatment capacities have developed. With this, the relative influence of extensive livestock rearing on BOD and FC concentrations in the Danube have increased.

https://doi.org/10.5194/gmd-2022-222
Preprint. Discussion started: 16 December 2022

Geoscientific Model Development
Discussions
Open Access

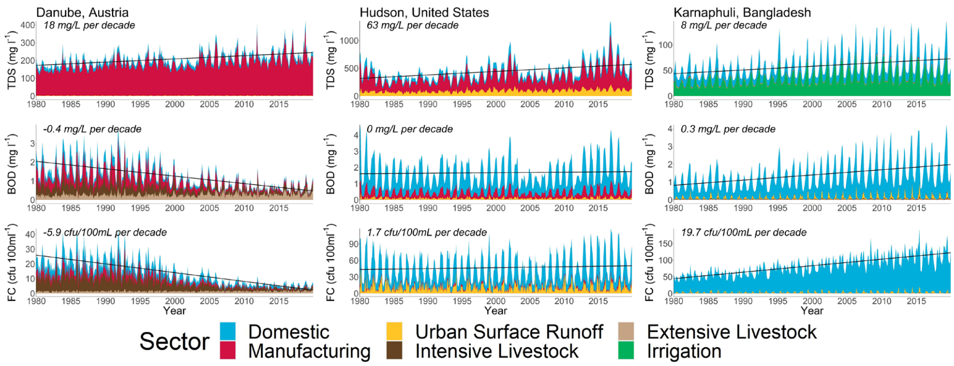

Figure 11. Simulated in-stream total dissolved solids (TDS; a), biological oxygen demand (BOD; b) and fecal coliform (FC; c) concentrations in selected rivers, disaggregated by contributing water use sectors and including linear decadal trends.

4. Discussion, conclusions and future work

To conclude, we have developed and evaluated a new global surface water quality model for simulating TDS, BOD and FC as indicators of salinity, organic and pathogen pollution, respectively. Building upon the water temperature model DynWat, and previous water quality model developments, the open-source code is structured in a way that allows for flexibility in both hydrological and pollutant loading inputs. Output data from DynQual has potential to inform assessments in a broad range of fields, including ecological, human health and water scarcity studies. Such work is relevant not only to the hydrological and water quality modelling communities, but also has applications for the broader scientific community in addition to informing policy regarding water resources management.

With few comparable studies in the current literature, it is difficult to assess the performance of DynQual relative to other large-scale surface water quality models. The quality of water temperature (Tw) simulations closely match those of the global water temperature models upon which DynQual is based (Van Vliet et al., 2012b; Wanders et al., 2019; Van Vliet et al., 2021). For total dissolved solids (TDS) and biological oxygen demand (BOD) concentrations, spatial patterns in normalised root mean square errors (nRMSE) are similar to previous work (Van Vliet et al., 2021), with reasonable model performance (<1 nRMSE) exhibited at monitoring locations across all continents. Other large-scale surface water quality models have validated simulated concentrations with respect to concentration classes linked to sectoral water use and environmental health limits. Following this approach, Wen et al., (2017) reported BOD concentrations simulated within the same classification in 94% of instances, however this is based on only 760 measurements of which 91% are modelled in the lowest pollutant class (0 – 5 mg l^{-1}). More comparable to our simulations, UNEP (2016) compared modelled and observed pollutant classes for TDS, BOD and fecal coliform (FC) concentrations across Latin America, Africa and Asia, achieving largely comparable model performance. It should be noted that while the validation data included by UNEP (2016) was derived exclusively from GEMStat, we expand our validation to include additional national datasets. While this further biases our validation towards countries with more extensive water quality observation networks (e.g. USA, Europe), this also allows for better consideration of the performance of DynQual over a wider range of hydrological conditions.

Uncertainties in water quality simulations arise from a combination of uncertainties associated with quantifications of pollutant loadings (e.g. pollutant excretion and emission rates), the quality of hydrological simulations (e.g. discharge and velocities) and the representation of in-stream processes (e.g. decay coefficients). Any model must also consider the trade-off between complexity and data availability (Weaver and Zwiers, 2000; Wen et al., 2017). Being a global model, DynQual is inherently unable to represent all aspects relevant to the local context. For example, a particular limitation is the lack of information on mining activities and road de-icing, which is relevant for TDS loadings. Furthermore, the representation of lakes and reservoirs in DynQual is rudimentary, with total (routed) loadings instantaneously averaged over the volume of the water body assuming full mixing. Lake mixing processes could be improved by including more detailed information on lake characteristics.

Our modelling strategy is thus to focus on the main spatial and temporal drivers of pollution in global river networks to facilitate first-order approximations of in-stream concentrations at high spatial (5 arc-min) and temporal (daily) resolution with global coverage. The model has particular value for simulating surface water quality in ungauged catchments and in facilitating projections of future surface water quality in the context of uncertain climatic and socio-economic changes. Future applications of DynQual may include: 1) expanding the number of modelled water quality constituents; 2) further spatio-temporal analysis of surface water quality, especially under hydro-meteorological extremes (droughts, heatwaves); and 3) investigating the impact of uncertain climatic and socio-economic change on future surface water quality.

5. Code and data availability

DynQual v1.0 is open source and distributed under the terms of the GNU General Public License version 3, or any later version, as published by the Free Software Foundation. The full model code, configuration INI files and a user manual is provided through a GitHub repository: https://githubv.com/UU-Hydro/DYNQUAL. The model code presented in this manuscript is archived at https://doi.org/10.5281/zenodo.7398411.

A full set-up with all required input datasets for running DynQual for the Rhine-Meuse basin is provided as an example (https://doi.org/10.5281/zenodo.7027242). Monthly water temperature (Tw) and salinity (TDS), organic (BOD) and pathogen (FC) concentrations are available directly via https://doi.org/10.5281/zenodo.7139222. Here, we also provide the output hydrological data (discharge and channel storage) simulated within the model run.

6. Author contribution

The research was designed by ERJ, MFPB and MTHvV. The surface water quality model was developed by ERJ, with assistance from NW and EHS. Output data analysis and presentation of results was led by ERJ, with guidance and feedback from MFPB, NW, LPHvB and MTHvV. All authors contributed to and approved the manuscript.

7. Competing interests

The authors declare no conflict of interest.

8. Acknowledgements

MTHvV was financially supported by a VIDI grant (Project No. VI.Vidi.193.019) of the Netherlands Scientific Organisation (NWO). NW acknowledges funding from NWO 016.Veni.181.049. We

https://doi.org/10.5194/gmd-2022-222
Preprint. Discussion started: 16 December 2022

Geoscientific Model Development Discussions
Open Access
EGU

acknowledge the Netherlands Organisation for Scientific Research (NWO) for the grant that enabled us to use the national supercomputer Snellius.

References

Beusen, A. H. W., Dekkers, A. L. M., Bouwman, A. F., Ludwig, W., and Harrison, J.: Estimation of global river transport of sediments and associated particulate C, N, and P, Global Biogeochemical Cycles, 19, 10.1029/2005gb002453, 2005.

Beusen, A. H. W., Van Beek, L. P. H., Bouwman, A. F., Mogollón, J. M., and Middelburg, J. J.: Coupling global models for hydrology and nutrient loading to simulate nitrogen and phosphorus retention in surface water – description of IMAGE–GNM and analysis of performance, Geosci. Model Dev., 8, 4045-4067, 10.5194/gmd-8-4045-2015, 2015.

Chapra, S. C. and Pelletier, G. J.: QUAL2K: A Modeling Framework for Simulating River and Stream Water Quality,

Cucchi, M., Weedon, G. P., Amici, A., Bellouin, N., Lange, S., Müller Schmied, H., Hersbach, H., and Buontempo, C.: WFDE5: bias-adjusted ERA5 reanalysis data for impact studies, Earth Syst. Sci. Data, 12, 2097-2120, 10.5194/essd-12-2097-2020, 2020.

Damania, R., Desbureaux, S., Rodella, A.-S., Russ, J., and Zaveri, E.: Quality Unknown: The Invisible Water Crises, World Bank Group, Washington, DC, 10.1596/978-1-4648-1459-4, 2019.

Ehalt Macedo, H., Lehner, B., Nicell, J., Grill, G., Li, J., Limtong, A., and Shakya, R.: Distribution and characteristics of wastewater treatment plants within the global river network, Earth Syst. Sci. Data, 14, 559-577, 10.5194/essd-14-559-2022, 2022.

Gudmundsson, L., Boulange, J., Do, H. X., Gosling, S. N., Grillakis, M. G., Koutroulis, A. G., Leonard, M., Liu, J., Müller Schmied, H., Papadimitriou, L., Pokhrel, Y., Seneviratne, S. I., Satoh, Y., Thiery, W., Westra, S., Zhang, X., and Zhao, F.: Globally observed trends in mean and extreme river flow attributed to climate change, Science, 371, 1159-1162, 10.1126/science.aba3996, 2021.

Hartmann, J., Lauerwald, R., and Moosdorf, N.: A Brief Overview of the GLObal RIver Chemistry Database, GLORICH, Procedia Earth and Planetary Science, 10, 23-27, https://doi.org/10.1016/j.proeps.2014.08.005, 2014.

Hofstra, N., Bouwman, A. F., Beusen, A. H. W., and Medema, G. J.: Exploring global Cryptosporidium emissions to surface water, Science of The Total Environment, 442, 10-19, https://doi.org/10.1016/j.scitotenv.2012.10.013, 2013.

Jones, E. R., van Vliet, M. T. H., Qadir, M., and Bierkens, M. F. P.: Country-level and gridded estimates of wastewater production, collection, treatment and reuse, Earth Syst. Sci. Data, 13, 237-254, 10.5194/essd-13-237-2021, 2021.

Jones, E. R., Bierkens, M. F. P., Wanders, N., Sutanudjaja, E. H., van Beek, L. P. H., and van Vliet, M. T. H.: Current wastewater treatment targets are insufficient to protect surface water quality, Communications Earth & Environment, 3, 221, 10.1038/s43247-022-00554-y, 2022.

Loucks, D. P. and Beek, E. v.: Water quality modeling and prediction, in: Water resource systems planning and management, Springer, 417-467, 2017.

Luthy, R. G., Sedlak, D. L., Plumlee, M. H., Austin, D., and Resh, V. H.: Wastewater-effluent-dominated streams as ecosystem-management tools in a drier climate, Frontiers in Ecology and the Environment, 13, 477-485, https://doi.org/10.1890/150038, 2015.

https://doi.org/10.5194/gmd-2022-222
Preprint. Discussion started: 16 December 2022

Ozaki, N., Fukushima, T., Harasawa, H., Kojiri, T., Kawashima, K., and Ono, M.: Statistical analyses on the effects of air temperature fluctuations on river water qualities, Hydrological Processes, 17, 2837-2853, https://doi.org/10.1002/hyp.1437, 2003.

Prüss-Ustün, A., Wolf, J., Bartram, J., Clasen, T., Cumming, O., Freeman, M. C., Gordon, B., Hunter, P. R., Medlicott, K., and Johnston, R.: Burden of disease from inadequate water, sanitation and hygiene for selected adverse health outcomes: An updated analysis with a focus on low- and middle-income countries, International Journal of Hygiene and Environmental Health, 222, 765-777, https://doi.org/10.1016/j.ijheh.2019.05.004, 2019.

Read, E. K., Carr, L., De Cicco, L., Dugan, H. A., Hanson, P. C., Hart, J. A., Kreft, J., Read, J. S., and Winslow, L. A.: Water quality data for national-scale aquatic research: The Water Quality Portal, Water Resources Research, 53, 1735-1745, https://doi.org/10.1002/2016WR019993, 2017.

Reder, K., Flörke, M., and Alcamo, J.: Modeling historical fecal coliform loadings to large European rivers and resulting in-stream concentrations, Environmental Modelling & Software, 63, 251-263, https://doi.org/10.1016/j.envsoft.2014.10.001, 2015.

Sirota, J., Baiser, B., Gotelli, N. J., and Ellison, A. M.: Organic-matter loading determines regime shifts and alternative states in an aquatic ecosystem, Proceedings of the National Academy of Sciences, 110, 7742-7747, doi:10.1073/pnas.1221037110, 2013.

Smucker, N. J., Beaulieu, J. J., Nietch, C. T., and Young, J. L.: Increasingly severe cyanobacterial blooms and deep water hypoxia coincide with warming water temperatures in reservoirs, Global Change Biology, 27, 2507-2519, https://doi.org/10.1111/gcb.15618, 2021.

Stefan, L., Christoph, M., Stephanie, G., Marco, C., Graham, P. W., Alessandro, A., Nicolas, B., Hannes Müller, S., Hans, H., Carlo, B., and Chiara, C.: WFDE5 over land merged with ERA5 over the ocean (W5E5 v2.0), 10.48364/ISIMIP.342217, 2021.

Sutanudjaja, E., Beek, R., Wanders, N., Wada, Y., Bosmans, J., Drost, N., Ent, R., de Graaf, I., Hoch, J., de Jong, K., Karssenberg, D., López, P., Pessenteiner, S., Schmitz, O., Straatsma, M., Vannametee, E., Wisser, D., and Bierkens, M.: PCR-GLOBWB 2: A 5 arcmin global hydrological and water resources model, Geoscientific Model Development, 11, 2429-2453, 10.5194/gmd-11-2429-2018, 2018.

Thomann, R. V. and Mueller, J. A.: Principles of surface water quality modeling and control, Harper & Row Publishers1987.

Thorslund, J. and van Vliet, M. T. H.: A global dataset of surface water and groundwater salinity measurements from 1980–2019, Scientific Data, 7, 231, 10.1038/s41597-020-0562-z, 2020.

Thorslund, J., Bierkens, M. F. P., Scaini, A., Sutanudjaja, E. H., and van Vliet, M. T. H.: Salinity impacts on irrigation water-scarcity in food bowl regions of the US and Australia, Environmental Research Letters, 17, 084002, 10.1088/1748-9326/ac7df4, 2022.

U.S. Geological Survey: National Water Information System data available on the World Wide Web (USGS Water Data for the Nation) [dataset], http://dx.doi.org/10.5066/F7P55KJN, 2016.

UNEP: A Snapshot of the World's Water Quality: Towards a global assessment, United Nations Environment Programme, Nairobi, Kenya, 162pp, 2016.

UNEP: GEMStat database of the Global Environment Monitoring System for Freshwater (GEMS/Water) Programme., 2020.

van Beek, L., Eikelboom, T., van Vliet, M., and Bierkens, M. F. P.: A physically based model of global freshwater surface temperature, Water Resources Research, 48, W09530, 10.1029/2012WR011819, 2012.

van Puijenbroek, P. J. T. M., Beusen, A. H. W., and Bouwman, A. F.: Global nitrogen and phosphorus in urban waste water based on the Shared Socio-economic pathways, Journal of Environmental Management, 231, 446-456, https://doi.org/10.1016/j.jenvman.2018.10.048, 2019.

van Vliet, M., Sheffield, J., Wiberg, D., and Wood, E.: Impacts of recent drought and warm years on water resources and electricity supply worldwide, Environmental Research Letters, 11, 124021, 10.1088/1748-9326/11/12/124021, 2016.

van Vliet, M., Yearsley, J., Ludwig, F., Vögele, S., Lettenmaier, D., and Kabat, P.: Vulnerability of US and European Electricity Supply to Climate Change, Nature Climate Change, 2, 676-681, 10.1038/nclimate1546, 2012a.

van Vliet, M., Franssen, W., Yearsley, J., Ludwig, F., Haddeland, I., Lettenmaier, D., and Kabat, P.: Global River Discharge and Water Temperature under Climate Change, Global Environmental Change, 23, 450-464, 10.1016/j.gloenvcha.2012.11.002, 2013.

van Vliet, M. T. H., Jones, E. R., Flörke, M., Franssen, W. H. P., Hanasaki, N., Wada, Y., and Yearsley, J. R.: Global water scarcity including surface water quality and expansions of clean water technologies, Environmental Research Letters, 16, 024020, 10.1088/1748-9326/abbfc3, 2021.

van Vliet, M. T. H., Yearsley, J. R., Franssen, W. H. P., Ludwig, F., Haddeland, I., Lettenmaier, D. P., and Kabat, P.: Coupled daily streamflow and water temperature modelling in large river basins, Hydrol. Earth Syst. Sci., 16, 4303-4321, 10.5194/hess-16-4303-2012, 2012b.

Velasco, J., Gutiérrez-Cánovas, C., Botella-Cruz, M., Sánchez-Fernández, D., Arribas, P., Carbonell, J. A., Millán, A., and Pallarés, S.: Effects of salinity changes on aquatic organisms in a multiple stressor context, Philosophical Transactions of the Royal Society B, 374, 20180011, 2019.

Virro, H., Amatulli, G., Kmoch, A., Shen, L., and Uuemaa, E.: GRQA: Global River Water Quality Archive, Earth Syst. Sci. Data, 13, 5483-5507, 10.5194/essd-13-5483-2021, 2021.

Voß, A., Alcamo, J., Bärlund, I., Voß, F., Kynast, E., Williams, R., and Malve, O.: Continental scale modelling of in-stream river water quality: a report on methodology, test runs, and scenario application, Hydrological Processes, 26, 2370-2384, https://doi.org/10.1002/hyp.9445, 2012.

Walton, N. R. G.: Electrical Conductivity and Total Dissolved Solids—What is Their Precise Relationship?, Desalination, 72, 275-292, https://doi.org/10.1016/0011-9164(89)80012-8, 1989.

Wanders, N. and Wada, Y.: Human and climate impacts on the 21st century hydrological drought, Journal of Hydrology, 526, 208-220, https://doi.org/10.1016/j.jhydrol.2014.10.047, 2015.

Wanders, N., van Vliet, M. T. H., Wada, Y., Bierkens, M. F. P., and van Beek, L. P. H.: High-Resolution Global Water Temperature Modeling, Water Resources Research, 55, 2760-2778, 10.1029/2018WR023250, 2019.

Weaver, A. and Zwiers, F.: Uncertainty in climate change, Nature, 407, 571-572, 10.1038/35036659, 2000.

Wen, Y., Schoups, G., and van de Giesen, N.: Organic pollution of rivers: Combined threats of urbanization, livestock farming and global climate change, Scientific Reports, 7, 43289, 10.1038/srep43289, 2017.

Wright, B., Stanford, B., Reinert, A., Routt, J., Khan, S., and Debroux, J.-F.: Managing water quality impacts from drought on drinking water supplies, Aqua, 63, 179, 10.2166/aqua.2013.123, 2014.

WWAP: The United Nations World Water Development Report 2017. Wastewater: The Untapped Resource, Paris, UNESCO, 2017.